J. Biochem. 2012;151(6):579–588 doi:10.1093/jb/mvs046

JB THE JOURNAL OF BIOCHEMISTRY

JB Review

Structural mechanism of disulphide bond-mediated redox switches

Received March 15, 2012; accepted April 13, 2012; published online May 2, 2012

Seong Eon Ryu*

Department of Bioengineering, College of Engineering, Hanyang University, 17 Haengdang-dong, Seongdong-gu, Seoul, Korea

* Tel: +82-2-2220-4020, Fax: +82-2-2220-4023, email: ryuse@hanyang.ac.kr

The oxidation of cysteine sulphydryl in proteins produces sulphenic acid that can form a reversible disulphide bond with another cysteine. The disulphide bond formation often triggers switches in protein structure and activity, especially when the distance between the two cysteine sulphur atoms is longer than the resulting disulphide bond distance. As an early example for the reversible disulphide bond-mediated functional switches, the reduced and oxidized forms of the bacterial transcription factor OxyR were characterized by X-ray crystallography. Recently, the *Drosophila* vision signalling protein, the association of inactivation-no-afterpotential D (INAD) was analysed by structural and functional methods. The two conserved cysteines of INAD were found to cycle between reduced and oxidized states during the light signal processing in *Drosophila* eyes, which was achieved by conformation dependent modulation of the disulphide bond redox potential. The production of the hypertension control peptide angiotensins was also shown to be controlled by the reversible disulphide bond in the precursor protein angiotensinogen. The crystal structure of the complex of angiotensiongen with its processing enzyme renin elucidated the role of the disulphide bond in stabilizing the precursor–enzyme complex facilitating the production of angiotensins. The increasing importance of the disulphide bond-mediated redox switches in normal and diseased states has implications in the development of novel antioxidant-based therapeutic approaches.

Keywords: redox switch/disulfide bond/OxyR/INAD/angiotensin.

Abbreviations: AMP-PNP, 5′-adenylylimidodiphosphate, a nonhydrolyzable ATP analog; PDZ, Post synaptic density protein-Drosophila disc large tumor suppressor-Zonula occludens-1 protein; UV/VIS, ultraviolet/visible.

Cells have evolved to develop a delicate network of regulatory pathways to deal with oxidative stresses that can potentially damage cellular materials (*1*). The cellular responses to oxidative conditions involve proteins such as transcription factors, signalling proteins, membrane channels and enzymes (*2*–*5*). Many of these redox-controlled proteins have cysteines that can be reversibly oxidized and the resulting modification of cysteines lead to activation or inhibition of the corresponding proteins' cellular function (*6*–*9*). The oxidized cysteine often forms reversible disulphide bond with another cysteine (*7*, *8*, *10*).

The sulphydryl group of cysteine has a unique reactivity towards oxidizing agents (*11*). The reactive oxygen species (ROS) modification of cysteine sulphydryl generates sulphenic, sulphinic or sulphonic acids (*12*), whereas the reactive nitrogen species (RNS) modification generates S-nitrosothiol (*13*, *14*) (Fig. 1). The redox active cysteine can be also glutathionylated (*15*) (Fig. 1). The sulphenic acid proceeds to the formation of disulphide bond either with a neighbouring cysteine in the corresponding protein or other cellular sulphydryls. Further oxidation of sulphenic acid to sulphinic or sulphonic acids cannot be reversed even in the presence of enough reductants. In a special case, the sulphinic acid formation in the peroxiredoxin active site can be reversed by an enzyme sulphiredoxin (*16*, *17*).

The oxidation-mediated disulphide bond formation within a protein was shown to induce structural switches (*8*). Although the extent of structural transition by a disulphide bond formation within a protein is dependent on the distance between two sulphur atoms, the structural transition often accompanies functional switches in proteins of transcription, signal transduction and heat shock responses. The disulphide bond-mediated structural switches can be more profound than those originated from phosphorylation. Phosphorylation of tyrosine or serine/throenine residues can trigger structural changes because the newly introduced phosphate group provides differences in charge and size of the corresponding amino acid side chain (*18*). In comparison, the disulphide bond switches provide a covalent modification between distant cysteines, which can bring distantly located cysteines into constrained positions, leading to a large conformational and functional switch in the protein.

Recently, structures of several disulphide bond switches were resolved by X-ray crystallography, which provided structural information on the diversity and significance of the disulphide bond-mediated redox switches. In this review, we focus on the redox switches in the *Drosophila* visual scaffold protein inactivation-no-afterpotential D (INAD) (*19*, *20*), the blood pressure controlling protein precursor angiotensinogen (*21*) and a couple of enzymes (*22*, *23*). Before the description of recent findings, we also briefly mention the OxyR redox switch (*24*, *25*) as an archetypal example of the disulphide bond-mediated redox switch. The discoveries described in this review indicate that there are common themes of the disulphide-mediated redox switches such as the

Featured Article

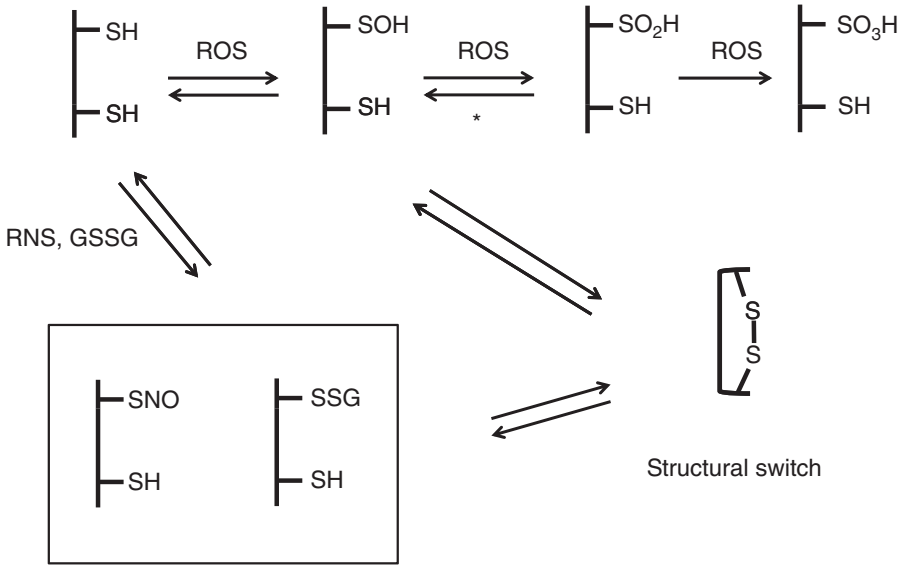

Fig. 1 Oxidative modification of cysteines and disulphide bond formation. Cysteine sulphydryl (SH) is sequentially oxidized by ROS to sulphenic acid (SOH), sulphinic acid (SO_2H) and sulphonic acid (SO_3H). The RNS and oxidized glutathione (GSSG) can oxidize cysteine sulphydryl to S-nitrosothiol (SNO) and glutathione disulphide bond (SSG). These oxidation intermediates can lead to the formation of disulphide bond and structural switches when the two sulphydryl distance is longer than the resulting disulphide bond distance. Asterisk indicates that the sulphinic acid formation in peroxiredoxins can be reversed to sulphenic acid by a specific enzyme sulphiredoxin.

structural transition-mediated functional switch, the conformation strain-driven switch mechanism and the transition time of millisecond range.

Reversible Disulphide Bond in the OxyR Transcription Factor

The *Escherichia coli* transcription factor OxyR, which is a member of the LysR family of bacterial transcription factors, is regulated by ROS modification (*26*). The activation of OxyR by ROS modification induces transcription of genes necessary for the defense of bacteria against harmful effects of ROS (*10*, *26*). The activation of OxyR involves a reversible disulphide bond formation between the conserved cysteines 199 and 208 starting from the oxidation of Cys199 to sulphenic acid (*10*). Biochemical studies including gel filtration, sedimentation and crosslinking experiments indicated that OxyR formed a tetramer in solution which appeared as a dimer of dimers (*27*). The DNase I footprinting studies revealed that the interactions between DNA and the OxyR tetramer were significantly different depending on whether OxyR was in reduced or oxidized state (*27*). The reduced and oxidized forms of OxyR exhibited different DNA sequence specificities.

The structure determination of OxyR in reduced form revealed that the two conserved cysteines 199 and 208 were distantly located with the inter-sulphur atom distance of ~17 Å (*24*). In the oxidized structure, the disulphide bond formation between the distant cysteines triggered a large conformational switch involving secondary structure rearrangements. The structural transition encompassed almost one entire face of the domain II of the OxyR regulatory domain.

In the reduced structure, the sulphydryl group of Cys199 pointed inwards the molecule occupying a mostly hydrophobic pocket formed by the inter-domain residues Ile98, Val101 and Ala147 (Fig. 2). Thus, the oxidation of Cys199 to sulphenic acid (Cys-OH) would destabilize the pocket geometry and induce the loop flipping out. The atoms on the 205–210 loop containing Cys208 had high thermal motion factors (B-factors) in the reduced structure, indicating that the region was flexible in the reduced state. The flexibility of the loop containing Cys208 facilitated the disulphide bond formation with the flipped-out Cys199 by increasing the chance of meeting between the two cysteines (Fig. 2). Upon disulphide bond formation of the two conserved cysteines, the short helix (αC) formed by residues 199–203 in the reduced structure disappeared. The extended strand (β8) of residues 219–222 became a helix-like structure. The flexible loop of residues 212–217 became a new β-strand (β8′).

The oxidation-mediated structural switch affected dimeric interface of OxyR, resulting in a relative rotation of monomers by ~30° compared to the monomers of the reduced-form dimer (*24*). The inter-monomer rotation in the dimer changed also the inter-dimer orientation in the tetramer and eventually the DNA interaction, which led to the induction of target genes. Mutations of the residues including I110D, H114Y, L124D and A233V which were supposed to disrupt the reduced-form dimeric interface, diminished DNA binding as assayed by the OxyR promoter repression (*28*). A homology model of full-length OxyR also indicated the domain rotation of OxyR and its role in DNA binding (*29*).

Kinetics of the OxyR Redox Switch

Although the crystal structures of reduced and oxidized OxyR explained structural mechanisms of the oxidation-mediated disulphide bond formation and subsequent functional transition (*24*), several questions

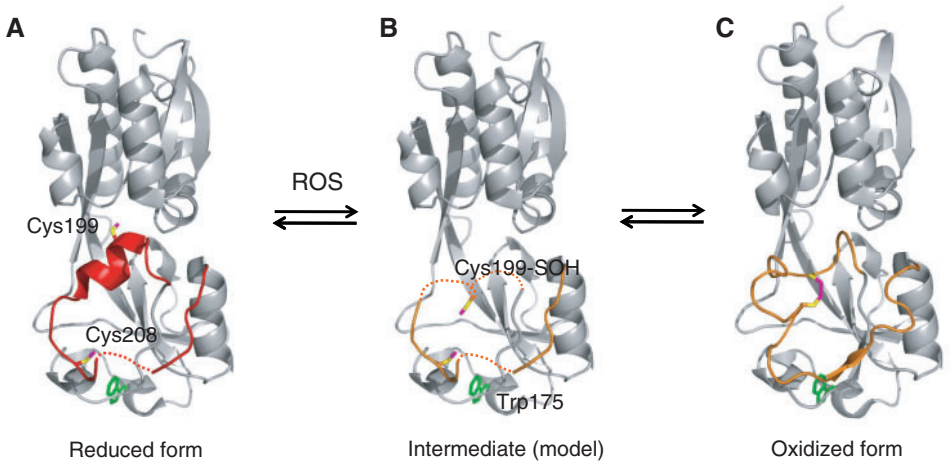

Fig. 2 The redox-dependent structural switches in OxyR. The reduced (A), intermediate (B) and oxidized forms (C) of OxyR were drawn in the figure. In the reduced form, the residues 195–204 were shown in red and side chains of two redox active cysteines 199 (located in the molecular centre) and 208 (located in the bottom of the molecule) were shown in magenta (sulphur atom) and yellow (C-beta carbon atom). The Trp175 generates fluorescence. When the primary redox active cysteine 199 was oxidized, the sulphenic acid (Cys199-SOH) was formed and ejected from the original hydrophobic pocket that could not fit the sulphenic acid. The Cys199-SOH ejection rendered the region flexible, and chance of meeting Cys 208 in another flexible loop was increased (B). When the Cys199 sulphenic acid met the Cys208 sulphydryl, disulphide bond was formed and secondary structural rearrangements occurred. In the intermediate and oxidized forms, the residues 195–204 region was shown in orange. The reduced and oxidized form structures were drawn from pdb codes 1I69 and 1I6A, respectively. The intermediate structure was modeled based on the reduced-form structure (pdb code: 1I69).

still remained. Those included the roles of the disulphide bond and its intermediates during oxidation of OxyR, and the forces driving the large structural switch. The extensive biochemical analyses including mass spectrometry, UV/Vis and fluorescence spectroscopy and stopped-flow kinetic analyses were carried out to answer the questions (*25*).

OxyR has six cysteines in the wild-type full-length state, complicating the analysis of the disulphide bond formation partners. For example, previous biochemical (*10*) and crystallographic studies (*24*) used the cysteine to alanine mutations (OxyR-4CA) in positions other than the disulphide bond-implicated Cys199 and Cys208. To resolve this complication, Lee *et al.* (*25*) used the wild-type OxyR with all six cysteine residues to show the specific disulphide bond between Cys199 and Cys208.

In addition, the conformation switch during the OxyR oxidation was analysed by the stopped-flow experiment using the large decrease in quantum yield of tryptophan fluorescence from Trp175 that is located near the loop containing Cys208 (*25*) (Fig. 2). The analysis indicated that the rate constant of the disulphide bond-mediated conformational switch was $\sim 9.7\,s^{-1}$. The rate is similar to that of ATP-induced allosteric transition in eukaryotic chaperonin CCT (10 and $17\,s^{-1}$ for two phases) (*30*). The value is also in the range of folding rate constants of some small proteins (*31*).

The driving force for the reduced to oxidized forms seems to be the flipping-out of the oxidized Cys199 from the hydrophobic inter-domain pocket and the flexibility of the loop containing Cys208 (*24*). However, the reverse reaction was not well understood. The analysis of conformational stability of both forms gave a clue to the mechanism of the reverse switch from the oxidized to reduced forms (*25*). Although the unfolding studies employing circular dichroism did not show differences between the reduced and oxidized OxyRs, the fluorescence spectroscopy by using the Trp175 fluorescence revealed that the oxidized state is destabilized by −3 kcal/mol compared to the reduced state OxyR. Thus, the local destabilization in the oxidized form appeared to mediate the reverse conformation switch once the disulphide bond was reduced. The strain-mediated structural switch is reminiscent of the conformational switch in serine protease inhibitors and the membrane fusion protein of influenza virus, where the strain loaded in the native form drives conformational transition (*32*, *33*).

Distinct redox agents appeared to generate different outputs in OxyR while modifying the same Cys199 (*34*). The modification with H_2O_2, GSSG and GSNO/S-nitrosocysteine formed sulphenic acid, a mixed disulphide bond and SNO, respectively. The helical content of OxyR varied between 52 and 78% depending on modification and the DNA binding affinity also exhibited significant differences. Although the different modifications may lead to different regulations of OxyR, the importance of disulphide bond-mediated structural switch seemed to be central in the regulation of OxyR because the mutation of Cys208, which was the partner of disulphide bond with Cys199, led to a significant decrease in the activity of OxyR (*10*). In addition, the oxidation of Cys199 by different oxidants also could eventually proceed to the formation of disulphide bond with Cys208 (*25*).

The Conformation-Coupled Redox Switch in the INAD Scaffold

Eukaryotic scaffold proteins play a pivotal role in cellular signal transduction by associating different proteins of the corresponding signalling pathways

(*35–37*). Concentration of signalling proteins by the association facilitates the signalling process by minimizing unwanted interactions with other proteins abundant in the cells. INAD is a *Drosophila* scaffold protein that assembles several components of visual signal transduction into a macromolecular complex in *Drosophila* photoreceptor neurons (*38–41*).

When the absorption of a photon of light occurs by rhodopsin a G-protein coupled receptor, the signal is conveyed to the sequential activation of a Gq isoform of heterotrimeric G protein and a phospholipase C (PLC-β) leading to the opening of transient receptor potential (TRP) channels in the microvilli membranes of the photoreceptor neurons. The TRP channel-mediated Ca^{2+} influx triggers both positive and negative feedback regulation of the *Drosophila* light signal transduction (*42*, *43*). The negative feedback is achieved by the eye specific protein kinase C (eye-PKC) (*43*, *44*). The scaffold protein INAD assembles the PLC-β, the TRP channel and eye-PKC through INAD's PDZ domains ensuring the high efficiency and speed of visual signalling (*45–48*).

The PDZ domain, which comprises 90–100 amino acid residues with a six-stranded β-sheet and two flanking α-helices, binds a ligand by using its surface groove formed by strand β2 and helix α2 (*49*, *50*). The crystal structure of the fifth PDZ domain (PDZ5, residues 580–665) of INAD revealed a disulphide bond between two conserved cysteines 606 and 645 (*19*). Although the overall structure of INAD PDZ5 was similar to other PDZ domains, a detailed comparison revealed significant deviations from the canonical PDZ structure, especially in the ligand binding site.

In the structure of INAD PDZ5 (*19*), the α1-helix was rotated ~70° relative to the corresponding helix in the canonical PDZ and most of the α2-helix is unwound. These structural changes significantly distorted the conformation of residues in helix α2 highly implicated in the ligand binding. The disulphide bond between Cys606 and Cys645 connected the β3-strand and the α2-helix, indicating that the disulphide bond formation was the cause of structural distortions in the ligand binding site. Measurement of the disulphide bond redox potential yielded a standard redox potential of −425 mV (*19*). Thus, in the cytosolic redox environment of cells with a redox potential of −230 to −300 mV (*51–54*), the PDZ5 cysteines were likely in the oxidized state. The reduced-form structure of PDZ5 (*19*), where the two cysteines were reduced by 10 mM DTT, exhibited the canonical PDZ domain structure. The inter-atomic distance between the two cysteine sulphur atoms was ~3.8 Å in the reduced structure, which was significantly longer than that of the oxidized structure with ~2.0 Å.

The PDZ5 disulphide bond formation *in vivo* was confirmed by the thiol-disulphide interconversion monitoring technique (*55*) with transgenic flies expressing wild-type INAD ($inaD^{wt}$) or the C645S mutant INAD ($inaD^{C645S}$) (*19*). The specific disulphide bond formation occurred in the $inaD^{wt}$ flies upon light exposure transiently, and the disulphide bond was reversed to the reduced state in the dark (*19*). Reception of single photons by wild-type photoreceptors produces transient electrical responses called quantum bumps through a coordinated opening of TRP channels (*42*). Although both the wild-type and $inaD^{C645S}$ photoreceptors exhibited normal quantum bumps, severe defects in the light response shutoff appeared in the $inaD^{C645S}$ mutant flies.

Thus, the oxidized form of INAD represented the off state of the light signalling and the dynamic cycling between the reduced and oxidized forms of INAD was essential for fast responses to the changing environment of light. Upon the transient darkening (~20 ms) experiment mimicking an approaching predator, the wild-type flies jumped to escape ~70% of the time, whereas the $inaD^{C645S}$ mutant flies did only ~10% (*19*). The behavioural defect was due to the mutant flies' disability to sense rapid decreases in light intensity, indicating that the reversible disulphide bond formation was essential in termination of light signal.

After the first structures of oxidized and reduced INAD proteins were published (*19*), further structural and functional studies were preformed to understand the detailed mechanism of the INAD redox switch (*20*). One of the major issues to address was as to how the light-dependent disulphide bond formation/breakage was achieved because it was expected that, *in vivo*, the redox potential of the environment surrounding the INAD-signalling complex would not fluctuate in large amplitude during the short timescale (about milliseconds) of the light signal transmission.

Despite the expectation of fast and reversible transition of disulphide bond between reduced and oxidized forms during the fly visual signalling, the isolated PDZ5 could not spontaneously cycle between the two forms. The redox potential of the Cys606–Cys645 disulphide bond of PDZ5 was lower than the redox potentials of cytosols in normal conditions (*19*, *51–54*). Thus, the two cysteines of PDZ5 are oxidized in cells and cannot cycle between reduced and oxidized forms in its isolated state.

In search of factors that enabled the disulphide bond reversibility, the interaction between PDZ domains 4 and 5 was found to play a critical role (*20*). The crystal structure determination of a INAD construct containing both PDZ4 and PDZ5 domains (PDZ45) revealed tight inter-domain interactions (*20*) (Fig. 3). The C-terminal residues of PDZ5 were extended from the body of the PDZ5 domain and bound to a groove on the PDZ4 domain, whose interactions further tightened the PDZ45 supramolecule (Fig. 3). In the structure of PDZ45 supramolecule, the PDZ5 domain exhibited the reduced cysteines 606 and 645, indicating that the tight domain interactions between PDZ4 and PDZ5 locked PDZ5 in its reduced state. Thus, the sulphydryls of Cys606 and Cys645 seemed to cycle between the reduced and oxidized states depending on the formation or uncoupling of the supramolecule between PDZ4 and PDZ5 domains.

Then, what triggers the uncoupling of PDZ4 and PDZ5 leading to the disulphide bond formation of PDZ5? Recently, it was found that a rapid and light-induced acidification occurred in fly microvilli due to protons released by PLCβ-mediated hydrolysis of PIP_2 (*56*). The PDZ4 and PDZ5 domain

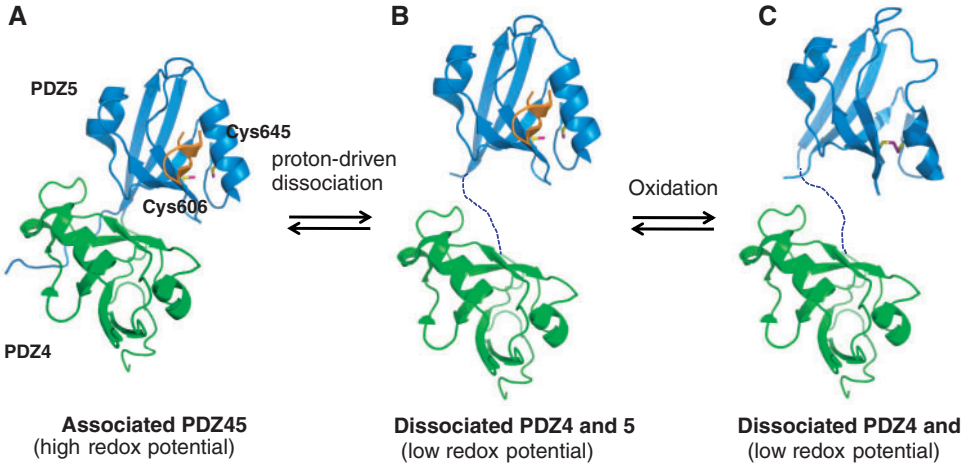

Fig. 3 Redox potential modulation in the INAD PDZ domains. The *Drosophila* visual signalling protein INAD cycles between the reduced and oxidized disulphide bond states of the PDZ5 domain (blue). In the dark state, the PDZ5 domain was associated with the PDZ4 domain (green) and the sulphydryls of the redox active cysteines 606 and 645 (sulphydryl in magenta) are in the reduced state (A, pdb code: 3R0H). The redox potential of cysteines in the associated state was high, and the two cysteines were stable in its reduced states. When the light signal was sensed, the proton was generated by an upstream process and triggered dissociation of the PDZ domains (B, a model based on pdb 3R0H). When the PDZ5 domain was dissociated, the redox potential of the two cysteines decreased significantly enough to form a disulphide bond in normal cytosolic redox environment [C, a model based on pdb 3R0H (PDZ4) and pdb 2QKT (oxidized PDZ5)]. The disulphide bond formation changed the structure of ligand binding pocket and the ligand (gold in A and B, a part of the target protein) was released to transmit the light signal. In B and C, the hypothetical connection between the two PDZ domains in the dissociated states is indicated as dashed lines.

interactions were shown to be uncoupled by the proton signal generated by hydrolysis of PIP2 by PLCβ in response to light via the Rhodopsin–Gα–PLCβ pathway (*20*). The proton signal appeared to protonate His547 of PDZ4 and disrupted its hydrogen-bond interaction with the C-terminal residue Thr669 of PDZ5, leading to the dissociation of the C-terminal loop of PDZ5 from the groove of PDZ4 and the uncoupling of the PDZ4 and PDZ5 domains.

The signal-dependent disulphide bond formation released the ligand (a part of the target protein) from PDZ5 whose ligand binding site had the optimal geometry for ligand binding only when the cysteines were reduced (Fig. 3). The conformation-coupled redox potential modulation seen in the INAD PDZ45 exhibits a novel example of active regulation of protein redox potential. Usually, proteins with redox machinery respond to environmental redox potential fluctuation or ROS signal (*4*, *57*). In comparison, the INAD PDZ45 changes its redox potential depending on the conformational status of domain interface, achieving the disulphide-mediated switch under almost constant cytosolic redox environment.

Modulation of Angiotensin Release in the Cardiovascular System

The vasopressor peptides angiotensins (*58*) are released by the enzymatic digestion of a serpin family protein angiotensinogen at its N-terminus (*59*, *60*). The proteolytic enzyme renin cleaves the peptide bond between the 10th and 11th amino acids of angiotensinogen to release the decapeptide angiotensin I that is further processed by the angiotensin converting enzyme (ACE) to produce the octapetide angiotensin II comprising the residues 1–8 of angiotensinogen (*58*, *61*).

A variety of studies for hypertension and its therapy were focused on ACE (*62–64*). In comparison, the release of angiotensins was regarded as a passive process by the enzyme action of renin. However, recent findings indicated that the enzyme digestion site was inaccessible in normal condition and became accessible only with the conformational rearrangements mediated by a conserved disulphide bond between cysteines 18 and 138 (*21*, *65*, *66*). The reversible disulphide bond of angiotensinogen in the N-terminal region was found to be important in the angiotensinogen's interaction with renin (*21*, *67*).

The crystal structure of the angiotensinogen–renin complex revealed that the complex formation preferred the oxidized form of angiotensinogen (*21*). In the structure, the N-terminal extention of angiotensinogen was detached from the body of the molecule and the cleavage site of angiotensinogen was located on the active site of renin (Fig. 4). The disulphide bond between Cys18 and Cys138 held the extension, providing conformational stability to the N-terminal extension residues. Otherwise the extension would be totally away from the molecular body and the correct interaction with renin may not be probable (Fig. 4).

The Cys18–Cys138 disulphide bond of angiotensinogen was labile and the redox potential of the disulphide bond was measured to be −230 mV (*21*). The oxidized form represented more constrained structure with a higher thermal stability of 62.6°C than the reduced form with a lower melting point of 57°C. In the plasma, the oxidized form of angiotensinogen was present in a ratio of 60:40 with the reduced form. The oxidized to reduced-form ratio was found to be highly preserved independent of gender or age (*21*). Despite the stable ratio in plasma, the ratio may change in focal tissues or vascular beds, leading to the reversible

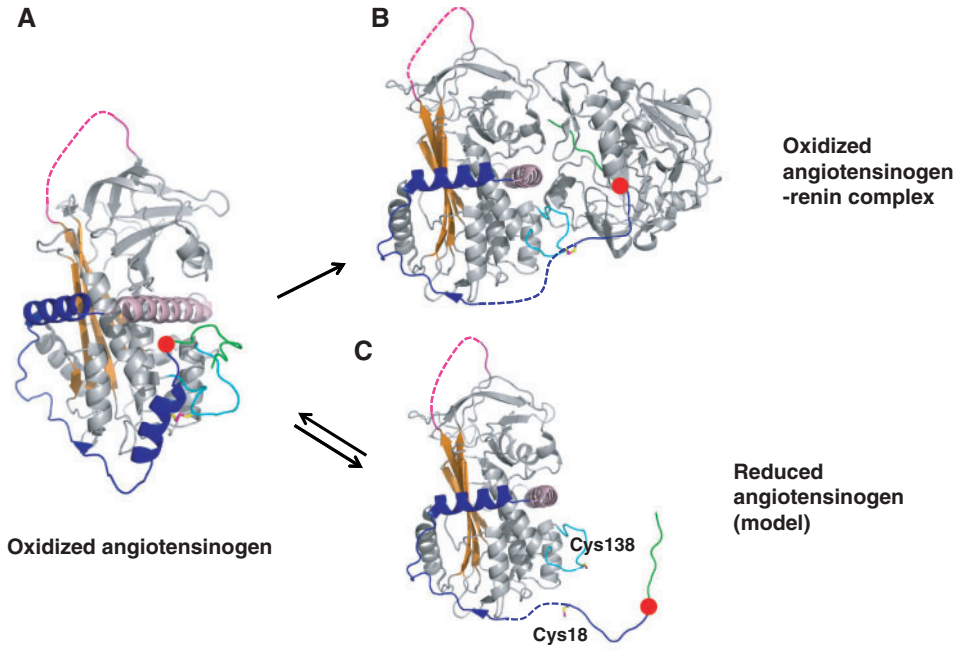

Fig. 4 Redox switch in the angiotensin release. The reversible disulphide bond of angiotensinogen between cysteines 18 and 138 (magenta) controls the production of angiotensin I that is the renin-cleaved N-terminal decapeptide (green). The oxidized angiotensinogen structure is drawn from pdb code 2WXW. ACE further processes the decapeptide yielding the octapeptide angiotensin II. The renin cleavage site is indicated as a red ball. The disulphide bond in oxidized angiotensinogen maintains the stability of N-terminal regions (green and blue) so that the cleavage site can fit into the active site of renin as shown in the oxidized angiotensinogen–renin complex (pdb code: 2X0B). In the modeled structure of reduced angiotensinogen where the disulphide bond was cleaved, and the N-terminal region was displaced in the *y*-direction from the original oxidized complex structure (pdb code: 2X0B), the N-terminal region is not maintained in an appropriate conformation for binding to the renin active site. Structurally unresolved regions are shown as dashed lines (magenta and blue).

switch between the oxidized and reduced forms. Thus, the redox environment of tissues would determine the rate and amount of angiotensin release, leading to the control of blood pressure.

The association of oxidative stress with the onset of episodic hypertension was observed previously (*68*, *69*). The oxidative stress-dependent conversion of angiotensiongen to the oxidized form leading to the production of angiotensins may explain the observation. Another example includes the oxidative stress due to the placental dysfunction (*70*, *71*). The affected individuals develop hypertension and pre-eclampsia, a leading cause of perinatal and maternal mortality and morbidity (*72–74*). The comparison of plasma samples of pregnant women with pre-eclampsia to the normal controls revealed that the diseased samples had decreased proportion of the reduced to oxidized angiotensinogen, indicating that the redox switch of angiotensinogen contributed to the hypertension and pre-eclampsia (*21*) and the antioxidant therapy could be effective in treatment of pre-eclampsia (*75*).

Redox Switches in Phosphatases and Kinases

Mitogen-activated protein kinase phosphatases (MKPs) are usually inactivated under oxidative stress, exerting positive control for the mitogen-activated protein kinase (MAPK) signalling by decreasing the dephosphorylation of activated MAPK (*76–80*). Other phosphatases such as PTP1B and PTEN sharing the similar active site structure with MKPs also are negatively regulated by oxidative conditions (*9*). In comparison to conventional MKPs and other phosphatases, the stress inducible MAPK phosphatase of yeast, Sdp1 acquires enhanced catalytic activity under oxidative conditions (*22*).

In response to oxidative stress, Sdp1 dephosphorylated activated Slt2 that was an essential protein in yeast's adaptation and survival over oxidative stress (*22*). Sdp1 also dephosphorylated the mammalian ERK2 MAPK that was a close relative of Slt2 (*81*, *82*). Optimal activity of Sdp1 was found to require a disulphide bond formation near the active site that was needed for selectively recognizing a tyrosine-phosphorylated MAPK substrate (*22*).

When the catalytic core domain (residues 56–197) of Sdp1 was expressed and analysed, there was no enzyme activity towards phosphor-ERK2, indicating that the N-terminal residues were crucial in the catalytic activity of Sdp1 (*22*). This is reminiscent of the N-terminal MAP kinase binding (MKB) domain (*78*). The MKB domain binds to the corresponding substrate kinases to provide specificity for the MKPs in the signal transduction (*83*). In comparison, the N-terminal sequences of Sdp1 supported the Sdp1 catalytic activity by using a cysteine residue (Cys 47) in the N-terminal sequences.

An *in vivo* analysis found that Cys47 formed disulphide bond with another conserved cysteine 142 under the oxidative stress. The physiological relevance was confirmed by analysing the *in vivo* redox state of

Sdp1 (*22*). When yeast cells were exposed to H_2O_2, the oxidized form of Sdp1 was detected in gels, whereas it was not with untreated cells. The crystal structure of Sdp1 (*22*) revealed that a disulphide bond between Cys47 and Cys142 was located near the catalytically active Cys 140, indicating that the disulphide bond formation was likely to affect substrate binding and enzyme activity.

Adenosine-5′-phosphosulphate (APS), APS reductase (APSR) and APS kinase (APSK) are essential components in the sulphur assimilation of *Arabidopsis* that converts the predominant form of environmental sulphur, inorganic sulphate (SO_4^{2-}) to physiologically useful forms such as sulphite, sulphide and cysteine (*84*, *85*). APSK is also essential for reproductive viability of *Arabidopsis* (*86–90*). In the crystal structure of *Arabidopsis thaliana* APSK (At-APSK), two conserved cysteines 86 and 119 formed an intersubunit disulphide bond in the dimeric structure (*23*).

The N-terminal region (residues 80–98) of one At-APSK monomer including Cys86 protruded from the main fold of the monomer and overlapped the other At-APSK monomer (*23*). The extended N-terminal region formed extensive interactions with the other monomer, and the intersubunit disulphide bond with Cys119 of the other domain stabilized the interactions. The location of the disulphide bond was relatively close to the binding sites of substrates APS and AMP-PNP, indicating that the disulphide bond formation should affect the enzyme activity. The At-APSK with reduced cysteines had 17-fold more efficient enzyme activity and 15-fold higher K_i value for APS than the oxidized form, indicating that the reversible disulphide bond formation functioned as a redox switch.

The redox-dependent modulation of APSK allows plants to control flux between the primary and secondary branches of sulphur assimilation. In the primary branch, APS is converted to sulphite by APSR, leading to generation of cysteine and glutathione. When the secondary pathway is activated, APSK is in function and converts APS to 3′-phospho-APS (PAPS) and eventually glucosinolates, hormones and phytosulphokines (*84*). Under oxidative stress conditions, there is an increasing demand for sulphur reduction to support glutathione synthesis. Then, the disulphide bond formation of APSK would increase, which results in inhibition of the secondary sulphur assimilation path and the synthesis of PAPS. The APSR, which promotes the primary metabolic pathway for the synthesis of cysteine and glutathione, is also known to be redox dependent (*91*). The disulphide bond formation activates APSR activity. Thus, oxidative stress in *Arabidopsis* and other plants controls the sulphur assimilation pathways by promoting and inhibiting two key enzymes in the primary and secondary metabolic pathways, respectively.

Perspectives

Numerous proteins are now known to be regulated by reversible disulphide bond formation. Recent examples indicate that there are different modes of the

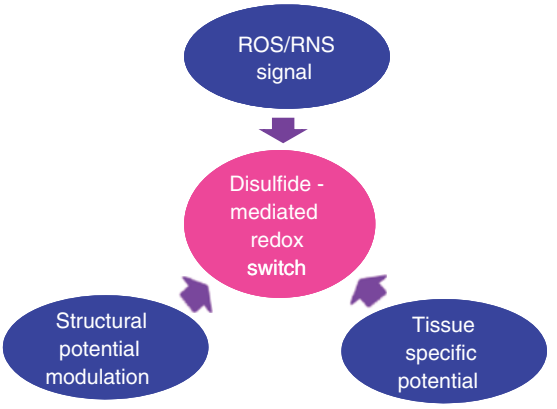

Fig. 5 Diverse modes of the disulphide bond-mediated redox switches. The disulphide-mediated redox switches are achieved by various ways including the ROS/RNS signal, the structural potential modulation switch and the tissue specific potential whose examples were seen in OxyR, INAD and antiotensinogen, respectively.

disulphide bond-mediated redox switches (Fig. 5). Although the detailed structural analysis has been limited to several examples, the common features of the disulphide bond-mediated redox switch proteins can be recognized from available examples. First, the reversible disulphide bond formation triggers the structural and functional switch. The extent of structural switch is dependent on how far the two redox active cysteines were originally located before the disulphide bond formation. OxyR's redox active cysteine sulphur atoms were 17 Å away to each other and their disulphide bond formation significantly refolded one face of OxyR. Flexibility of the cysteine-containing loop contributes to the disulphide bond formation between the distant cysteines. In the case of INAD, the inter-sulphur atom distance in the reduced form was greater than the disulphide bond length in the oxidized form. Both in OxyR and INAD, the disulphide bond-mediated structural switch in the local area affected allosteric interactions in domain interfaces, leading to the proteins' functional modulation.

Second, the disulphide bond formation changes protein structure stability, which can exert a driving force for the structural switch and the redox potential modulation. In OxyR case, the folding stability measurement revealed that there was a local conformational strain in the oxidized form that could drive the transition from the oxidized to reduced form. The disulphide bond formation seemed to stabilize the INAD PDZ5 domain considering that the PDZ5 domain is readily oxidized and have a low redox potential. The reduced-form structure was locked by domain interaction between PDZ4 and PDZ5, indicating that the domain interaction provided the necessary stability to maintain the reduced-form structure. In angiotensinogen also, the thermal stability was different between the oxidized and reduced forms.

Third, the timescales of the structural transition are milliseconds. The stopped-flow experiments revealed that the conformation switch rate in OxyR was $\sim 9.7\,s^{-1}$ (transition time: 103 ms). Although the rate was not measured in other cases, the time needed to respond to light in the INAD complex was 20–30 ms,

indicating that the conformation switch in INAD occurred in the millisecond range. The millisecond timescale was previously observed in an allosteric structural transition of eukaryotic chaperonin CCT (*30*). The transition time was a little longer in OxyR because the OxyR transition appeared to proceed in two steps (*25*).

There are other proteins that could not be covered in this review. Those include succinic semialdehyde dehydrogenase (SSADH) (*92*) and *trans*-activating response DNA-binding protein of 43 kDa (TDP-43) (*9*) and others. They have similar redox switch mechanisms described in this review. As structures of more disulphide bond-mediated proteins are resolved, one could see a confirmation of general features as well as novel mechanisms. With the current and future novel discoveries, it is certain that the importance of the disulphide bond-mediated control of protein functions will increase in both normal and diseased physiological conditions, which has implications for the development of new therapeutic approaches. For example, the antioxidant treatment for patients with pre-eclampsia may decrease the angiotensin release rate and hypertension.

Funding

This study was supported by a Hanyang University internal grant and a biomedical technology grant from the National Research Foundation of Korea.

Conflict of interest

None declared.

References

1. Imlay, J.A. (2003) Pathways of oxidative damage. *Annu. Rev. Microbiol.* **57**, 395–418
2. Imlay, J.A. (2008) Cellular defenses against superoxide and hydrogen peroxide. *Annu. Rev. Biochem.* **77**, 755–776
3. Finkel, T. (2011) Signal transduction by reactive oxygen species. *J. Cell Biol* **194**, 7–15
4. Rhee, S.G. (2006) Cell signaling. H2O2, a necessary evil for cell signaling. *Science* **312**, 1882–1883
5. Miki, H. and Funato, Y. (2012) Regulation of intracellular signalling through cysteine oxidation by reactive oxygen species. *J. Biochem.* **151**, 255–261
6. Barford, D. (2004) The role of cysteine residues as redox-sensitive regulatory switches. *Curr. Opin. Struct. Biol.* **14**, 679–686
7. Brandes, N., Schmitt, S., and Jakob, U. (2009) Thiol-based redox switches in eukaryotic proteins. *Antioxid. Redox Signal* **11**, 997–1014
8. Antelmann, H. and Helmann, J.D. (2011) Thiol-based redox switches and gene regulation. *Antioxid. Redox Signal* **14**, 1049–1063
9. Ostman, A., Frijhoff, J., Sandin, A., and Bohmer, F.D. (2011) Regulation of protein tyrosine phosphatases by reversible oxidation. *J. Biochem.* **150**, 345–356
10. Zheng, M., Aslund, F., and Storz, G. (1998) Activation of the OxyR transcription factor by reversible disulfide bond formation. *Science* **279**, 1718–1721
11. Reddie, K.G. and Carroll, K.S. (2008) Expanding the functional diversity of proteins through cysteine oxidation. *Curr. Opin. Chem. Biol.* **12**, 746–754
12. Hugo, M., Turell, L., Manta, B., Botti, H., Monteiro, G., Netto, L.E., Alvarez, B., Radi, R., and Trujillo, M. (2009) Thiol and sulfenic acid oxidation of AhpE, the one-cysteine peroxiredoxin from *Mycobacterium tuberculosis*: kinetics, acidity constants, and conformational dynamics. *Biochemistry* **48**, 9416–9426
13. Forrester, M.T., Foster, M.W., Benhar, M., and Stamler, J.S. (2009) Detection of protein S-nitrosylation with the biotin-switch technique. *Free Radic. Biol. Med* **46**, 119–126
14. Hess, D.T., Matsumoto, A., Kim, S.O., Marshall, H.E., and Stamler, J.S. (2005) Protein S-nitrosylation: purview and parameters. *Nat. Rev. Mol. Cell Biol.* **6**, 150–166
15. Martinez-Ruiz, A. and Lamas, S. (2007) Signalling by NO-induced protein S-nitrosylation and S-glutathionylation: convergences and divergences. *Cardiovasc. Res.* **75**, 220–228
16. Lowther, W.T. and Haynes, A.C. (2011) Reduction of cysteine sulfinic acid in eukaryotic, typical 2-Cys peroxiredoxins by sulfiredoxin. *Antioxid. Redox Signal* **15**, 99–109
17. Rhee, S.G., Jeong, W., Chang, T.S., and Woo, H.A. (2007) Sulfiredoxin, the cysteine sulfinic acid reductase specific to 2-Cys peroxiredoxin: its discovery, mechanism of action, and biological significance. *Kidney Int. Suppl.* **106**, S3–S8
18. Deshmukh, L., Meller, N., Alder, N., Byzova, T., and Vinogradova, O. (2011) Tyrosine phosphorylation as a conformational switch: a case study of integrin beta3 cytoplasmic tail. *J. Biol. Chem.* **286**, 40943–40953
19. Mishra, P., Socolich, M., Wall, M.A., Graves, J., Wang, Z., and Ranganathan, R. (2007) Dynamic scaffolding in a G protein-coupled signaling system. *Cell* **131**, 80–92
20. Liu, W., Wen, W., Wei, Z., Yu, J., Ye, F., Liu, C.H., Hardie, R.C., and Zhang, M. (2011) The INAD scaffold is a dynamic, redox-regulated modulator of signaling in the Drosophila eye. *Cell* **145**, 1088–1101
21. Zhou, A., Carrell, R.W., Murphy, M.P., Wei, Z., Yan, Y., Stanley, P.L., Stein, P.E., Broughton Pipkin, F., and Read, R.J. (2010) A redox switch in angiotensinogen modulates angiotensin release. *Nature* **468**, 108–111
22. Fox, G.C., Shafiq, M., Briggs, D.C., Knowles, P.P., Collister, M., Didmon, M.J., Makrantoni, V., Dickinson, R.J., Hanrahan, S., Totty, N., Stark, M.J., Keyse, S.M., and McDonald, N.Q. (2007) Redox-mediated substrate recognition by Sdp1 defines a new group of tyrosine phosphatases. *Nature* **447**, 487–492
23. Ravilious, G.E., Nguyen, A., Francois, J.A., and Jez, J.M. (2012) Structural basis and evolution of redox regulation in plant adenosine-5′-phosphosulfate kinase. *Proc. Natl Acad. Sci. USA* **109**, 309–314
24. Choi, H., Kim, S., Mukhopadhyay, P., Cho, S., Woo, J., Storz, G., and Ryu, S.E. (2001) Structural basis of the redox switch in the OxyR transcription factor. *Cell* **105**, 103–113
25. Lee, C., Lee, S.M., Mukhopadhyay, P., Kim, S.J., Lee, S.C., Ahn, W.S., Yu, M.H., Storz, G., and Ryu, S.E. (2004) Redox regulation of OxyR requires specific disulfide bond formation involving a rapid kinetic reaction path. *Nat. Struct. Mol. Biol.* **11**, 1179–1185
26. Storz, G., Tartaglia, L.A., and Ames, B.N. (1990) Transcriptional regulator of oxidative stress-inducible genes: direct activation by oxidation. *Science* **248**, 189–194

27. Toledano, M.B., Kullik, I., Trinh, F., Baird, P.T., Schneider, T.D., and Storz, G. (1994) Redox-dependent shift of OxyR-DNA contacts along an extended DNA-binding site: a mechanism for differential promoter selection. *Cell* **78**, 897–909
28. Kullik, I., Toledano, M.B., Tartaglia, L.A., and Storz, G. (1995) Mutational analysis of the redox-sensitive transcriptional regulator OxyR: regions important for oxidation and transcriptional activation. *J. Bacteriol.* **177**, 1275–1284
29. Zaim, J. and Kierzek, A.M. (2003) The structure of full-length LysR-type transcriptional regulators. Modeling of the full-length OxyR transcription factor dimer. *Nucleic Acids Res.* **31**, 1444–1454
30. Kafri, G. and Horovitz, A. (2003) Transient kinetic analysis of ATP-induced allosteric transitions in the eukaryotic chaperonin containing TCP-1. *J. Mol. Biol.* **326**, 981–987
31. Grantcharova, V., Alm, E.J., Baker, D., and Horwich, A.L. (2001) Mechanisms of protein folding. *Curr. Opin. Struct. Biol.* **11**, 70–82
32. Lee, C., Park, S.H., Lee, M.Y., and Yu, M.H. (2000) Regulation of protein function by native metastability. *Proc. Natl Acad. Sci. USA* **97**, 7727–7731
33. Carr, C.M. and Kim, P.S. (1993) A spring-loaded mechanism for the conformational change of influenza hemagglutinin. *Cell* **73**, 823–832
34. Kim, S.O., Merchant, K., Nudelman, R., Beyer, W.F. Jr, Keng, T., DeAngelo, J., Hausladen, A., and Stamler, J.S. (2002) OxyR: a molecular code for redox-related signaling. *Cell* **109**, 383–396
35. Bhattacharyya, R.P., Remenyi, A., Yeh, B.J., and Lim, W.A. (2006) Domains, motifs, and scaffolds: the role of modular interactions in the evolution and wiring of cell signaling circuits. *Annu. Rev. Biochem.* **75**, 655–680
36. Morrison, D.K. and Davis, R.J. (2003) Regulation of MAP kinase signaling modules by scaffold proteins in mammals. *Annu. Rev. Cell Dev. Biol.* **19**, 91–118
37. Schoch, S., Castillo, P.E., Jo, T., Mukherjee, K., Geppert, M., Wang, Y., Schmitz, F., Malenka, R.C., and Sudhof, T.C. (2002) RIM1alpha forms a protein scaffold for regulating neurotransmitter release at the active zone. *Nature* **415**, 321–326
38. Huber, A. (2001) Scaffolding proteins organize multimolecular protein complexes for sensory signal transduction. *Eur. J. Neurosci.* **14**, 769–776
39. Montell, C. (2005) TRP channels in Drosophila photoreceptor cells. *J. Physiol.* **567**, 45–51
40. Tsunoda, S. and Zuker, C.S. (1999) The organization of INAD-signaling complexes by a multivalent PDZ domain protein in Drosophila photoreceptor cells ensures sensitivity and speed of signaling. *Cell Calcium* **26**, 165–171
41. Hardie, R.C. and Raghu, P. (2001) Visual transduction in Drosophila. *Nature* **413**, 186–193
42. Henderson, S.R., Reuss, H., and Hardie, R.C. (2000) Single photon responses in Drosophila photoreceptors and their regulation by Ca^{2+}. *J. Physiol* **524**, Pt 1, 179–194
43. Ranganathan, R., Harris, G.L., Stevens, C.F., and Zuker, C.S. (1991) A Drosophila mutant defective in extracellular calcium-dependent photoreceptor deactivation and rapid desensitization. *Nature* **354**, 230–232
44. Smith, D.P., Ranganathan, R., Hardy, R.W., Marx, J., Tsuchida, T., and Zuker, C.S. (1991) Photoreceptor deactivation and retinal degeneration mediated by a photoreceptor-specific protein kinase C. *Science* **254**, 1478–1484
45. Chevesich, J., Kreuz, A.J., and Montell, C. (1997) Requirement for the PDZ domain protein, INAD, for localization of the TRP store-operated channel to a signaling complex. *Neuron* **18**, 95–105
46. Huber, A., Sander, P., Gobert, A., Bahner, M., Hermann, R., and Paulsen, R. (1996) The transient receptor potential protein (Trp), a putative store-operated Ca^{2+} channel essential for phosphoinositide-mediated photoreception, forms a signaling complex with NorpA, InaC and InaD. *EMBO J.* **15**, 7036–7045
47. Shieh, B.H., Zhu, M.Y., Lee, J.K., Kelly, I.M., and Bahiraei, F. (1997) Association of INAD with NORPA is essential for controlled activation and deactivation of Drosophila phototransduction in vivo. *Proc. Natl Acad. Sci. USA* **94**, 12682–12687
48. Tsunoda, S., Sierralta, J., Sun, Y., Bodner, R., Suzuki, E., Becker, A., Socolich, M., and Zuker, C.S. (1997) A multivalent PDZ-domain protein assembles signalling complexes in a G-protein-coupled cascade. *Nature* **388**, 243–249
49. Doyle, D.A., Lee, A., Lewis, J., Kim, E., Sheng, M., and MacKinnon, R. (1996) Crystal structures of a complexed and peptide-free membrane protein-binding domain: molecular basis of peptide recognition by PDZ. *Cell* **85**, 1067–1076
50. Hung, A.Y. and Sheng, M. (2002) PDZ domains: structural modules for protein complex assembly. *J. Biol. Chem.* **277**, 5699–5702
51. Hanson, G.T., Aggeler, R., Oglesbee, D., Cannon, M., Capaldi, R.A., Tsien, R.Y., and Remington, S.J. (2004) Investigating mitochondrial redox potential with redox-sensitive green fluorescent protein indicators. *J. Biol. Chem.* **279**, 13044–13053
52. Hwang, C., Lodish, H.F., and Sinskey, A.J. (1995) Measurement of glutathione redox state in cytosol and secretory pathway of cultured cells. *Methods Enzymol.* **251**, 212–221
53. Keese, M.A., Saffrich, R., Dandekar, T., Becker, K., and Schirmer, R.H. (1999) Microinjected glutathione reductase crystals as indicators of the redox status in living cells. *FEBS Lett.* **447**, 135–138
54. Ostergaard, H., Tachibana, C., and Winther, J.R. (2004) Monitoring disulfide bond formation in the eukaryotic cytosol. *J. Cell Biol* **166**, 337–345
55. Leichert, L.I. and Jakob, U. (2004) Protein thiol modifications visualized in vivo. *PLoS Biol.* **2**, e333
56. Huang, J., Liu, C.H., Hughes, S.A., Postma, M., Schwiening, C.J., and Hardie, R.C. (2010) Activation of TRP channels by protons and phosphoinositide depletion in Drosophila photoreceptors. *Curr. Biol.* **20**, 189–197
57. Janssen-Heininger, Y.M., Mossman, B.T., Heintz, N.H., Forman, H.J., Kalyanaraman, B., Finkel, T., Stamler, J.S., Rhee, S.G., and van der Vliet, A. (2008) Redox-based regulation of signal transduction: principles, pitfalls, and promises. *Free Radic. Biol. Med.* **45**, 1–17
58. Fyhrquist, F. and Saijonmaa, O. (2008) Renin-angiotensin system revisited. *J. Intern. Med.* **264**, 224–236
59. Stein, P.E., Tewkesbury, D.A., and Carrell, R.W. (1989) Ovalbumin and angiotensinogen lack serpin S-R conformational change. *Biochem. J.* **262**, 103–107
60. Huber, R. and Carrell, R.W. (1989) Implications of the three-dimensional structure of alpha 1-antitrypsin for

structure and function of serpins. *Biochemistry* **28**, 8951–8966
61. Dickson, M.E. and Sigmund, C.D. (2006) Genetic basis of hypertension: revisiting angiotensinogen. *Hypertension* **48**, 14–20
62. Koga, H., Yang, H., Adler, J., Zimmermann, E.M., and Teitelbaum, D.H. (2008) Transanal delivery of angiotensin converting enzyme inhibitor prevents colonic fibrosis in a mouse colitis model: development of a unique mode of treatment. *Surgery* **144**, 259–268
63. Altin, T., Kilickap, M., Tutar, E., Turhan, S., Atmaca, Y., Gulec, S., Oral, D., and Erol, C. (2007) The relationship of chronic angiotensin converting enzyme inhibitor use and coronary collateral vessel development. *Int. Heart J.* **48**, 435–442
64. Sherman, R.C. and Langley-Evans, S.C. (1998) Early administration of angiotensin-converting enzyme inhibitor captopril, prevents the development of hypertension programmed by intrauterine exposure to a maternal low-protein diet in the rat. *Clin. Sci.* **94**, 373–381
65. Kobori, H., Nangaku, M., Navar, L.G., and Nishiyama, A. (2007) The intrarenal renin-angiotensin system: from physiology to the pathobiology of hypertension and kidney disease. *Pharmacol. Rev.* **59**, 251–287
66. Nguyen, G., Delarue, F., Burckle, C., Bouzhir, L., Giller, T., and Sraer, J.D. (2002) Pivotal role of the renin/prorenin receptor in angiotensin II production and cellular responses to renin. *J. Clin. Invest.* **109**, 1417–1427
67. Streatfeild-James, R.M., Williamson, D., Pike, R.N., Tewksbury, D., Carrell, R.W., and Coughlin, P.B. (1998) Angiotensinogen cleavage by renin: importance of a structurally constrained N-terminus. *FEBS Lett.* **436**, 267–270
68. Wilcox, C.S. (2005) Oxidative stress and nitric oxide deficiency in the kidney: a critical link to hypertension? *Am. J. Physiol. Regul. Integr. Comp. Physiol.* **289**, R913–R935
69. Harrison, D.G. and Gongora, M.C. (2009) Oxidative stress and hypertension. *Med. Clin. North Am.* **93**, 621–635
70. Myatt, L. (2010) Review: reactive oxygen and nitrogen species and functional adaptation of the placenta. *Placenta* **31 (Suppl)**, S66–S69
71. Burton, G.J. and Jauniaux, E. (2004) Placental oxidative stress: from miscarriage to preeclampsia. *J. Soc. Gynecol. Investig.* **11**, 342–352
72. Hubel, C.A. (1999) Oxidative stress in the pathogenesis of preeclampsia. *Proc. Soc. Exp. Biol. Med.* **222**, 222–235
73. Sedeek, M., Gilbert, J.S., LaMarca, B.B., Sholook, M., Chandler, D.L., Wang, Y., and Granger, J.P. (2008) Role of reactive oxygen species in hypertension produced by reduced uterine perfusion in pregnant rats. *Am. J. Hypertens.* **21**, 1152–1156
74. Mistry, H.D., Wilson, V., Ramsay, M.M., Symonds, M.E., and Broughton Pipkin, F. (2008) Reduced selenium concentrations and glutathione peroxidase activity in preeclamptic pregnancies. *Hypertension* **52**, 881–888
75. Hoffmann, D.S., Weydert, C.J., Lazartigues, E., Kutschke, W.J., Kienzle, M.F., Leach, J.E., Sharma, J.A., Sharma, R.V., and Davisson, R.L. (2008) Chronic tempol prevents hypertension, proteinuria, and poor feto-placental outcomes in BPH/5 mouse model of preeclampsia. *Hypertension* **51**, 1058–1065
76. Ikner, A. and Shiozaki, K. (2005) Yeast signaling pathways in the oxidative stress response. *Mutat. Res.* **569**, 13–27
77. Chang, L. and Karin, M. (2001) Mammalian MAP kinase signalling cascades. *Nature* **410**, 37–40
78. Keyse, S.M. (2000) Protein phosphatases and the regulation of mitogen-activated protein kinase signalling. *Curr. Opin. Cell Biol.* **12**, 186–192
79. Tonks, N.K. (2005) Redox redux: revisiting PTPs and the control of cell signaling. *Cell* **121**, 667–670
80. Salmeen, A. and Barford, D. (2005) Functions and mechanisms of redox regulation of cysteine-based phosphatases. *Antioxid. Redox Signal* **7**, 560–577
81. Hahn, J.S. and Thiele, D.J. (2002) Regulation of the Saccharomyces cerevisiae Slt2 kinase pathway by the stress-inducible Sdp1 dual specificity phosphatase. *J. Biol. Chem.* **277**, 21278–21284
82. Collister, M., Didmon, M.P., MacIsaac, F., Stark, M.J., MacDonald, N.Q., and Keyse, S.M. (2002) YIL113w encodes a functional dual-specificity protein phosphatase which specifically interacts with and inactivates the Slt2/Mpk1p MAP kinase in S. cerevisiae. *FEBS Lett.* **527**, 186–192
83. Tao, X. and Tong, L. (2007) Crystal structure of the MAP kinase binding domain and the catalytic domain of human MKP5. *Protein Sci.* **16**, 880–886
84. Patron, N.J., Durnford, D.G., and Kopriva, S. (2008) Sulfate assimilation in eukaryotes: fusions, relocations and lateral transfers. *BMC Evol. Biol.* **8**, 39
85. Marzluf, G.A. (1997) Molecular genetics of sulfur assimilation in filamentous fungi and yeast. *Annu. Rev. Microbiol.* **51**, 73–96
86. Mugford, S.G., Lee, B.R., Koprivova, A., Matthewman, C., and Kopriva, S. (2011) Control of sulfur partitioning between primary and secondary metabolism. *Plant J.* **65**, 96–105
87. Mugford, S.G., Yoshimoto, N., Reichelt, M., Wirtz, M., Hill, L., Mugford, S.T., Nakazato, Y., Noji, M., Takahashi, H., Kramell, R., Gigolashvili, T., Flugge, U.I., Wasternack, C., Gershenzon, J., Hell, R., Saito, K., and Kopriva, S. (2009) Disruption of adenosine-5′-phosphosulfate kinase in Arabidopsis reduces levels of sulfated secondary metabolites. *Plant Cell* **21**, 910–927
88. Kopriva, S., Mugford, S.G., Matthewman, C., and Koprivova, A. (2009) Plant sulfate assimilation genes: redundancy versus specialization. *Plant Cell Rep.* **28**, 1769–1780
89. Mugford, S.G., Matthewman, C.A., Hill, L., and Kopriva, S. (2010) Adenosine-5′-phosphosulfate kinase is essential for Arabidopsis viability. *FEBS Lett.* **584**, 119–123
90. Yatusevich, R., Mugford, S.G., Matthewman, C., Gigolashvili, T., Frerigmann, H., Delaney, S., Koprivova, A., Flugge, U.I., and Kopriva, S. (2010) Genes of primary sulfate assimilation are part of the glucosinolate biosynthetic network in Arabidopsis thaliana. *Plant J.* **62**, 1–11
91. Bick, J.A., Setterdahl, A.T., Knaff, D.B., Chen, Y., Pitcher, L.H., Zilinskas, B.A., and Leustek, T. (2001) Regulation of the plant-type 5′-adenylyl sulfate reductase by oxidative stress. *Biochemistry* **40**, 9040–9048
92. Kim, Y.G., Lee, S., Kwon, O.S., Park, S.Y., Lee, S.J., Park, B.J., and Kim, K.J. (2009) Redox-switch modulation of human SSADH by dynamic catalytic loop. *EMBO J.* **28**, 959–968